XVIII International Conference on Water Resources
CMWR 2010
J. Carrera (Ed)
CIMNE, Barcelona 2010

# PREDICTION OF RESIDUAL OIL SATURATION IN MIXED-WET NETWORKS USING ACCURATE PORE SHAPE DESCRIPTORS

**Andrey V. Ryazanov, Marinus I.J. van Dijke and Kenneth S. Sorbie**

Institute of Petroleum Engineering,
Heriot-Watt University, Edinburgh EH14 4AS, UK
e-mail: andrey.ryazanov@pet.hw.ac.uk, web page: http://www.pet.hw.ac.uk

**Key words:** Network modelling, two-phase flow, non-uniform wettability, oil layers, residual oil saturation, pore-shape characterization

**Summary.** Immobilization of non-aqueous phase liquids (NAPL) is similar to oil trapping during waterflooding in oil reservoirs. Proper two-phase flow simulation, including trapped or residual oil saturation, requires accurate capillary pressure and relative permeabilities curves. Pore-scale network modelling can be used to estimate these flow parameters.

The present two-phase pore network modelling tool takes as input geometrically and topologically representative networks from digital pore space reconstructions to generate the corresponding flow curves. Recently, Ryazanov at el.[1] have included the thermodynamic oil layers collapse criterion[2] in this network model. In this work, a new n-cornered star shape characterization technique (*Star*)[3] has been implemented in addition to the commonly used Circle-arbitrary Triangle-Square (*CTS*) shape representation.

The *BereaCT* network, extracted from a 3D CT image has been used for a number of sensitivities of the waterflood residual oil saturation, relative permeabilities and for matching experimental water-wet data, using both the *CTS* and the *Star* approaches. It has been shown that shape approximations (*CTS* or *Star*) and oil layers collapse criterion have a significant impact on the residual oil and the relative permeabilities. Both approximations gave very good agreement with the experimental drainage curves, but the *Star* approach gave a better match of the imbibition curves compared to *CTS*.

## 1 INTRODUCTION

Simulation of two-phase flow processes with immobilization NAPL or oil trapping requires accurate descriptions of the capillary pressures and relative permeabilities. Pore-scale network modelling is an attractive tool for estimating these flow parameters.

For each pore-level displacement during a two phase flooding cycle, a capillary entry pressure is required. The so-called MS-P method is normally used for calculating the entry pressures in non-circular capillaries. An overview of the literature corresponding to this theory is given by Lago and Araujo[4]. The above references have only considered capillaries of uniform wettability. However, only part of the pore surface may change wettability and a model for this wettability alteration is described by Kovscek et al.[5]. To explain the experimental observation that, after water invasion, the oil residual can be quite low, Kovscek proposed that oil layers are sandwiched between water corner films and bulk water in the centre of pores. A literature overview of non-uniform wettability entry pressures derivation, oil layer theory and experimental observations can be found in van Dijke and Sorbie[2].

Blunt[6] actually described the formation and collapse of these layers in a pore with square cross-section and assumed that the layers would collapse when the surrounding oil–water interfaces met and derived the corresponding geometrical collapse criteria (*Geom*). Many

authors have used these criteria for formation and collapse of layers in capillary bundles[7, 8] and network models[6, 9-12]. However, Blunt's collapse criteria are purely geometrical and are not based on a firm thermodynamic argument. Recently, van Dijke and Sorbie[2] developed thermodynamically based criteria for the existence of oil layers (*Therm*). These criteria are consistent with the MS-P capillary entry pressures for other water invasion displacements and are more restrictive than the geometrical collapse criteria.

In this work, we use a two-phase pore network model, recently developed by Ryazanov et al.[1], who have included the thermodynamic oil layers collapse criteria[2] in it. In that model, a new n-cornered star (*Star*) shape characterization technique has been implemented in addition to the commonly used Circle-arbitrary Triangle-Square (*CTS*) shape representation[1, 3]. For numerical calculations we consider the network extracted from Berea sandstone with the different shape characterization (*Star*, *CTS*). We perform a wide range of network model sensitivity calculations of residual oil saturation to various fractionally-wet wettability conditions and analyze the effect of pore shape characterization on $S_{or}$ behavior.

Additionally, we examine the sensitivity of relative permeability to average advancing contact angle and to oil-wet fraction. We also investigate the effect of oil layer existence criteria and pore shape characterization on the relative permeability curves. To validate the pore-scale network model, the calculated relative permeabilities for both shape approximations are compared with water-wet experiments.

## 2 NETWORK MODELLING

### 2.1 Network model description

The newly developed pore-network modelling tool is similar in certain respects to models found in the literature[12-14] in that it takes as input the geometrically and topologically equivalent network extracted from a real pore space. The network consists of pores bodies (nodes) and pore throats (bonds) for which the characteristic properties (radius, volume, shape factor, inscribed and hydraulic radii etc) have been derived from the original sample. The data structure for these unstructured networks has been described by Bakke and Øren[15] and Piri and Blunt[11]. Note that in addition to previously used pore properties, we also use the hydraulic radius, when available, as an additional parameter to characterize pore shapes using n-cornered stars[3].

For the model simulations in this paper we consider network derived from Berea sandstone sample. The network has been extracted from a micro–computer 3D tomography image, using a new enhanced extraction technique[16].

### 2.2 Pore-shape characterization (CTS, Star)

#### *C-T-S Shape Characterization*

The most common approach is to represent the pore cross section shape by a circle, an (irregular) triangle or a square (*C-T-S*) with a shape factor that matches that of the real pore shape[12-14]. The shape factor is defined as $G = A/L^2$, where $A$ and $L$ are the area and perimeter of the cross section, respectively. The disadvantage of *C-T-S* is that these shapes are all convex, while a significant fraction of pore shapes are usually non-convex. Convexity can be indicated by the ratio of the hydraulic radius $R_h$ and the inscribed radius $R_{ins}$ of the cross section, the dimensionless hydraulic radius $H=R_h/R_{ins}=(A/L)/R_{ins}$. If $H<0.5$ a shape is non-convex, while convex shapes have $H\geq 0.5$. For the circle, square and arbitrary triangle $H=0.5$.

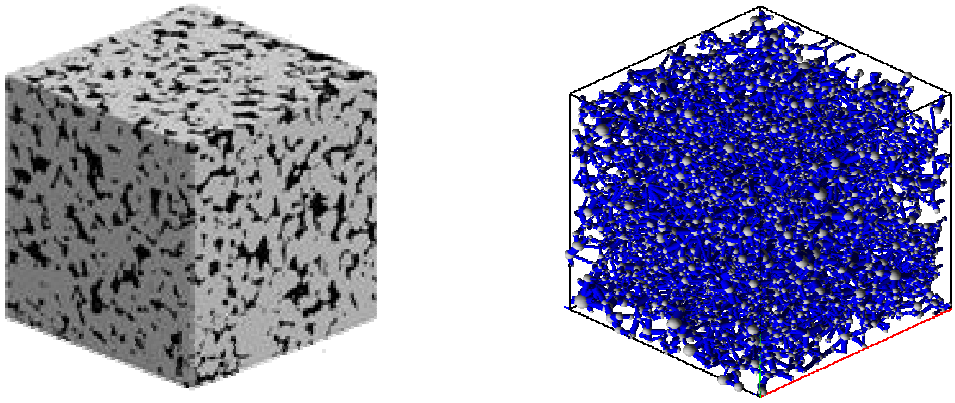

(a) (b)

Figure 1: (a) 3D CT image of Berea sandstone sample; (b) Network extracted from 3D CT image of Berea sandstone sample (*BereaCT*)[16]

***N-cornered Star Shape Characterization***

The regular n-cornered star shape, can be used to represent non-convex shapes, contrary to the arbitrary triangle. The regular star has two parameters, the number of corners n and the corner half-angle $\gamma$. For any cross section with dimensionless hydraulic radius $H$<0.5 and arbitrary shape factor $G$, a star can be uniquely identified[3].

### 2.3 Displacement processes

All pore fluid configurations and displacements for primary drainage and water invasion have been described in the previous work [1], except so called pore body filling (*PBF*) events[17] which have been reported by Blunt[18].

## 3 RESULTS AND DISCUSSION

### 3.1 Network for Berea sandstone (CTS, Star)

The *BereaCT* network, extracted from a 3D CT image of Berea sandstone sample has been used for a number of sensitivities and predicting experimental data: The pore space image and the corresponding extracted network is shown in Figure 1. The main parameters of the network are given in Table 1. Both the *CTS* and the *Star* approaches have been used for pore shape representation.

### 3.2 Sensitivity studies

To analyze the effect of wettability on residual oil saturation and relative permeabilities we consider a series of different wettability distributions for network *BereaCT*. During drainage the network is assumed to be water-wet with drainage contact angle $\theta_{dr}$ uniformly distributed between 0 and 60 degrees. After aging the advancing contact angles $\theta_a$ of the oil-contacted parts of the oil-filled pores are taken according to a fractionally wet distribution (FWD) with six values of oil-wet fractions

$$\alpha_j = 0.5 + 0.1(j-1),\ j = 1..6 \tag{1}$$

and for each of those $\alpha_j$ values we define nine ranges of advancing contact angles

$$\theta_a \in \left[\theta_a^i - 5, \theta_a^i + 5\right],\ \theta_a^i = 95 + 10(i-1),\ i = 1..9. \quad (2)$$

We characterize each case by the pair of values $(\alpha_j, \theta_a^i)$. For all sensitivity cases we have simulated primary drainage and secondary waterflooding with ageing included after drainage.

| Network | *BereaCT* | |
|---|---|---|
| Shape characterization | *STAR* | *C-T-S* |
| Circle (%) | 0.4 | 1.1 |
| Arb. Triangle (%) | 22.8 | 71.8 |
| Square (%) | 0.5 | 27.1 |
| N-Star (%) | 76.3 | 0.0 |
| Number of nodes | 7776 | |
| Number of bonds | 14475 | |
| Coordination number | 3.69 | |
| Permeability, mD | 1595.18 | 1699.26 |
| Net Porosity, % | 18.98 | |
| Clay Bound Porosity, % | 5.6 | |

Table 1: Main network parameters

***Residual oil saturation***

The residual oil saturations $S_{or}$ are presented against the average advancing contact angle $\theta_a^i$ for the different oil-wet fractions $\alpha$ (Figure 2(a,b)). The residual oil behavior is in agreement with previous findings for the uniformly oil-wet case ($\alpha$=1), where pore bodies were excluded from the displacement process[1]. Here, the pore bodies are included explicitly in the flooding process and they are allowed to experience the same type of displacements as the pore throats, as well as *PBF* events in the case of spontaneous displacement.

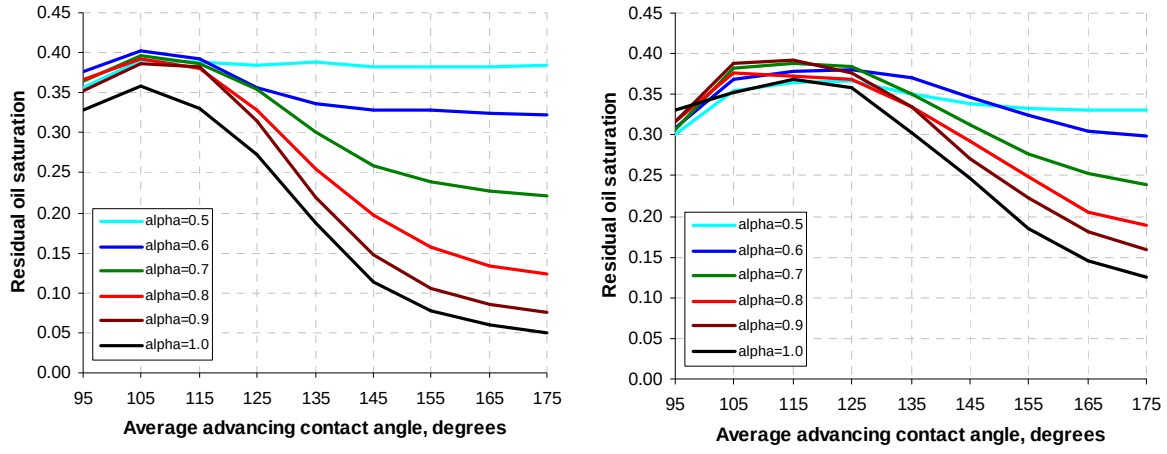


(a) (b)

Figure 2: Residual oil saturation sensitivity (*BereaCT* network) to oil-wet fraction $\alpha$ and average advancing contact angle $\theta_a^i$; (a) – *CTS* approach, (b) – *Star* approach.

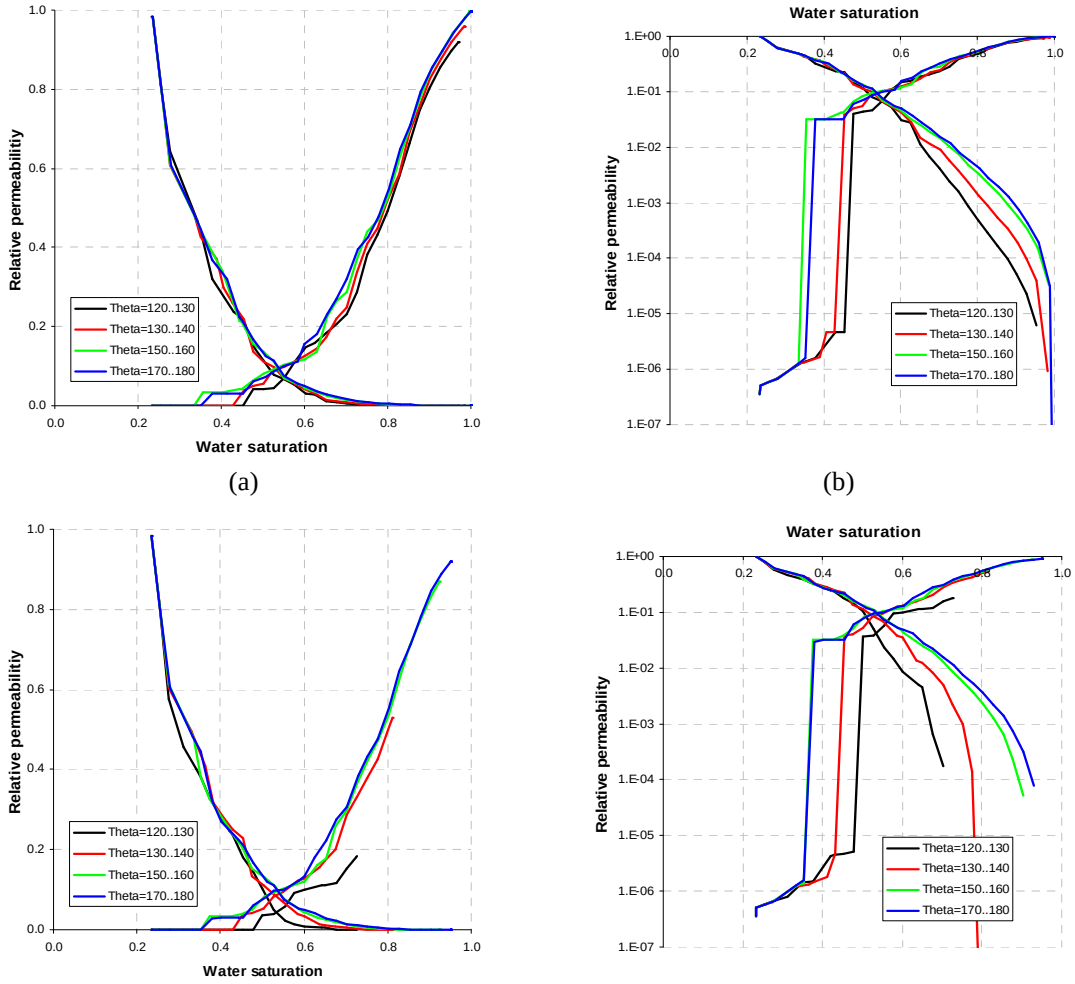


Figure 3: Sensitivity of relative permeabilities to average advancing contact angle with oil-wet fraction $\alpha$=1.0 (*BereaCT* network). (a,b) – *CTS* approach with *Geom* criterion, (c,d) – *CTS* approach with *Therm*

The residual oil saturation decreases with increasing average contact angle (beyond $\theta_a^i$ of around 115 degrees) with the more rapid decline for the higher oil-wet fraction values (Figure 2(a,b)). This can be explained by the increasing presence of oil layers during the waterflooding cycle, which improve oil phase continuity and result in better oil recovery[1]. For the weakly oil-wet cases ($\theta_a^i$ between 95 and 115 degrees) the number of snap-off displacements increases as the contact angle increases, but the very small number of oil layers formation events is not enough to compensate for the reduction of oil phase continuity and this results in a slightly increasing residual.

Modelling pore shapes by *Star* (Figure 2(b)), rather than by *CTS* (Figure 2(a)), has a large effect on the residual oil saturations for the larger contact angles. The residual oil variation range for *Star* is narrower compared to *CTS*. This can be explained from the presence of more arbitrary triangular shapes for *CTS* than for the *Star* case (Table 1). And since the drainage contact angle is distributed over a wide range, $\theta_{dr} \in [0, 60]$, there will be a higher fraction of arbitrary triangles without corner water films after the drainage (at least in the largest corners) than for the star shapes. After aging, if the corners without water films become oil-wet then

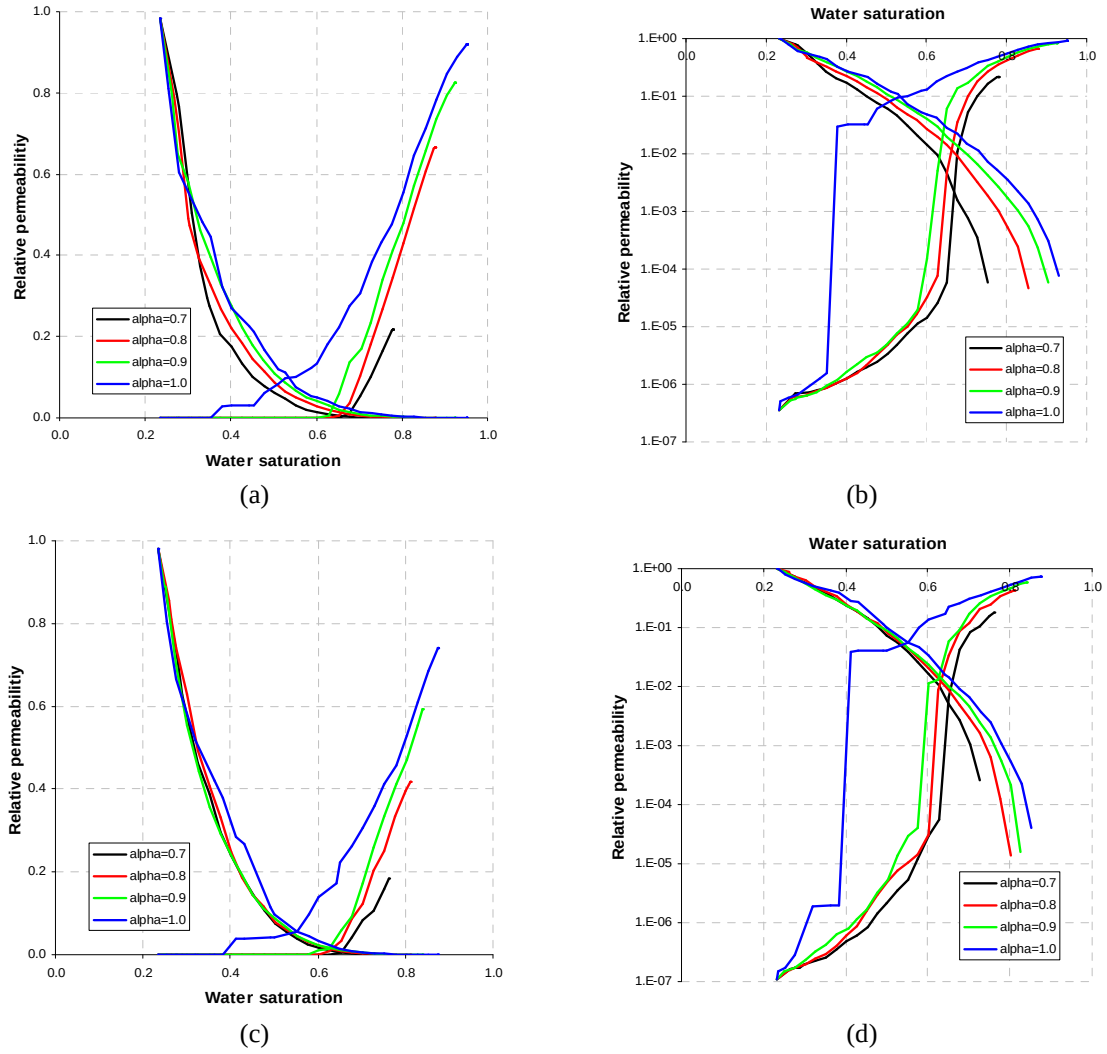


Figure 4: Sensitivity of relative permeabilities to oil-wet fraction for strongly oil-wet pores (BereaCT network, *Therm* layers criterion). (a,b) – *CTS* approach, (c,d,) – *Star* approach.

during the waterflooding it could have more stable oil wetting films, which maintains the oil continuity better than oil layers.

***Relative permeabilities***

To show the effect of wettability on the water flood relative permeability curves we have considered two sensitivities for the *BereaCT* network: 1) sensitivity to average advancing contact angle $\theta_a^i$ for a uniformly oil-wet system ($\alpha$=1.0) (Figure 3). 2) sensitivity to oil-wet fraction $\alpha$ with the strongly oil-wet advancing contact angle distribution $\theta_a \in$ [170,180] (Figure 4).

For sensitivity 1 we have calculated relative permeabilities for the *CTS* approach with the *Geom* (Figure 3(a,b)) and *Therm* (Figure 3(c,d)) oil layers existence criteria. First, the less restrictive oil layers existence criterion *Geom* produces lower $S_{or}$[1] and higher $K_{rw}$ end-points (Figure 3(a,b)) compared to the more restrictive Therm criterion (Figure 3(c,d)). The $K_{rw}$ curves for Geom are very similar for all values of $\theta_a^i$, at the higher $S_w$, while for Therm the

$K_{rw}$ curves increase gradually with $\theta_a^i$.

For all cases, $K_{ro}$ increases with $\theta_a^i$ (Figure 3(b,d)) at high $S_w$. This is the result of increased oil phase conductivity due to existence of many oil layers. Similarly, $K_{rw}$ increases with $\theta_a^i$ at low $S_w$. Nevertheless, the crossover of the $K_{rw}$ and $K_{ro}$ curves hardly shifts to lower $S_w$ with increasing oil-wetness.

For sensitivity 2, we have calculated relative permeabilities for the *Therm* criteria with *CTS* (Figure 4(a,b)) and *Star* (Figure 4(c,d)) approximation. Contrary to sensitivity 1, the relative permeability crossover shows a significant shift towards low $S_w$, as the oil-wet fraction $\alpha$ increases. The $K_{ro}$ curves have two opposite trends as $\alpha$ increases: a decrease at low $S_w$ values and an increase at high $S_w$ values. At the start of the water flood, displacements occur in the small water-wet pores, followed by displacements in the large oil-wet pores. For increasing fractions of oil-wet pores $\alpha$ the latter displacements start earlier during the flood, which explains the decrease of $K_{ro}$ at low $S_w$. On the other hand, for decreasing $\alpha$ (more water wet pores) we have more pore body filling events occurring at higher water saturations, resulting in more trapped oil clusters which do not contribute to $K_{ro}$. Thus, for higher $S_w$ the trend changes and $K_{ro}$ increases with $\alpha$.

The *Star* curves (Figure 4 (c,d)) show lower $K_{rw}$, lower end-point $K_{rw}$ and higher $S_{or}$ compared to the corresponding *CTS* curves. This is a consequence of the larger number of arbitrary triangular shapes in *CTS* than in *Star*, leading to more stable corner films instead of oil layers, as explained above.

| Network | | *BereaCT* |
|---|---|---|
| Contact angle, degrees | Drainage | $\theta_{dr}$ =0 |
| | Imbibition | $\theta_a$ =36..56 |
| Connate water saturation | | 0.20 |

Table 2: Input parameters used for prediction of Oak's water-wet experiments

### 3.3 Comparison Network simulations with experimental data

To investigate the effect of pore shape characterization on the prediction of experiments we have made comparisons with Oak's water-wet experiments for Berea sandstone[19]. For the *BereaCT* network we have considered the two pore shape approximations *CTS* and *Star*. The wettability scenario is presented in Table 2. Relative permeability predictions for both pore shape approximations show very good agreement with the experimental drainage curves, but the *Star* approach gives a better match of the imbibition curves compared to *CTS*, as the latter overestimates the $K_{ro}$ (Figure 5). This illustrates the superiority of the *Star* over the *CTS* approach.

## 4. SUMMARY AND CONCLUSIONS

Recently, Ryazanov at el.[1] have included a full thermodynamically based oil layer existence and collapse model (*Therm*) in a two-phase pore network simulator. The *Therm* layer model is more restrictive than the previously used geometrical criteria (*Geom*). In the network model, a new n-cornered star (*Star*) shape characterization technique has been implemented, in addition to the commonly used Circle-arbitrary Triangle-Square (*CTS*) shape representation. The *BereaCT* network, extracted from a 3D CT image has been used for a

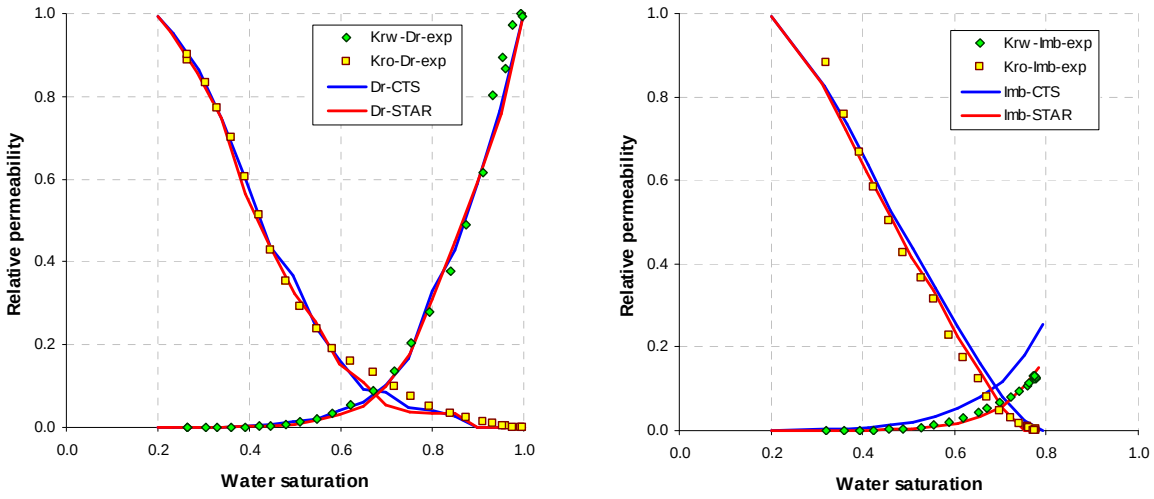


(a) (b)

Figure 5: Comparison of predicted relative permeabilities for Drainage (a) and Imbibition (b) with Oak's data for *BereaCT* network (*Star* vs *CTS*)

number of sensitivities of the waterflood residual oil saturation, relative permeabilities and for matching experimental water-wet data. Both the *CTS* and the *Star* approach have been used.

The sensitivity of residual oil saturation $S_{or}$ to the average advancing contact angle $\theta_a^i$ for different oil-wet fractions $\alpha$ has been investigated. $S_{or}$ decreases with increasing average contact angle with a more rapid decline for the higher oil-wet fraction values and $S_{or}$ decreases with increasing oil-wet fraction. Modelling pore shapes by *Star*, rather than by *CTS*, has a significant effect on $S_{or}$ for the larger contact angles, as the $S_{or}$ range for *Star* is narrower compared to that for *CTS*.

Two sensitivities of relative permeability have been performed: 1) sensitivity to average advancing contact angle for a uniformly oil-wet system, *CTS* with *Geom* and *Therm* criterion; 2) sensitivity to oil-wet fraction with the strongly oil-wet advancing contact angle distribution, *CTS* and *Star* with *Therm* criterion. For sensitivity 1, the less restrictive oil layers existence criteria *Geom* produces lower $S_{or}$ and higher $K_{rw}$ end-points compared to the more restrictive *Therm* criteria. The $K_{rw}$ curves for *Geom* are very similar for all values of the advancing contact angles at the higher $S_w$, while for *Therm* the $K_{rw}$ curves increase gradually with contact angle. For sensitivity 2, contrary to sensitivity 1, the relative permeability crossover shows a significant shift towards low $S_w$, as the oil-wet fraction increases. The $K_{ro}$ curves have two opposite trends as the oil-wet fraction increases: a decrease at low $S_w$ values and an increase at high $S_w$ values. The *Star* curves show lower $K_{rw}$, lower end-point $K_{rw}$ and higher $S_{or}$ compared to the corresponding *CTS* curves.

We have considered the two pore shape approximations *CTS* and *Star* to match Oak's data[19]. Both approximations give very good agreement with the drainage curves, but the *Star* approach gives a better match of the imbibition curves compared to *CTS*.

However, the most important contribution is that this paper introduces a new model of oil trapping in systems of arbitrary wettability by incorporating the correct physics of oil layer existence and collapse. This improves our understanding of how residual oil is formed or how NAPL becomes immobilized. Nevertheless, the present idealization of the real 3D pore shapes using straight tubes with angular cross-sections may still not predict residual saturations accurately. In addition, this paper shows that wettability has a large effect on

residual oil saturation. However, deriving the precise pore-scale characterization of wettability from experiments remains a challenge.

## ACKNOWLEDGMENTS

Support for Andrey Ryazanov was provided through the Dorothy Hodkins scholarship of the EPSRC. The authors also thank Dr. Kejian Wu and Dr. Zeyun Jiang for providing *BereaCT* network data for us.

## REFERENCES

[1] A Ryazanov, MIJ van Dijke and KS Sorbie, "Two-Phase Pore-Network Modelling: Existence of Oil Layers During Water Invasion", *Transport in Porous Media*, **80**(1), 79-99 (2009).

[2] M.I.J. van Dijke and K.S. Sorbie, "Existence of fluid layers in the corners of a capillary with non-uniform wettability", *J. Coll. Int. Sci.*, **293**(2), 455-463 (2006).

[3] J. O. Helland, A. V. Ryazanov and M. I. J. Van Dijke, "Characterization of pore shapes for pore network models", In Proceedings of the 11th European Conference on the Mathematics of Oil Recovery (ECMOR XI), *Bergen, Norway*, September (2008).

[4] M. Lago and M. Araujo, "Threshold pressure in capillaries with polygonal cross section", *Journal of Colloid and Interface Science*, **243**(1), 219-226 (2001).

[5] A.R. Kovscek, H. Wong and C.J. Radke, "A Pore-Level Scenario for the Development of Mixed Wettability in Oil Reservoirs", *AIChE Journal*, **39**, 1072-1085 (1993).

[6] M. J. Blunt, "Pore level modeling of the effects of wettability", *SPE J*, **2**(4), 494-510 (1997).

[7] M. H. Hui and M. J. Blunt, "Effects of wettability on three-phase flow in porous media", *Journal of Physical Chemistry B*, **104**(16), 3833-3845 (2000).

[8] J. O. Helland and S. M. Skjaeveland, "Physically based capillary pressure correlation for mixed-wet reservoirs from a bundle-of-tubes model", *SPE J*, **11**(2), 171-180 (2006).

[9] P.E. Øren, S. Bakke and O.J. Arntzen, "Extending predictive capabilities to network models", *SPE J*, **3**(4), 324-336 (1998).

[10] M. Piri and M.J. Blunt, "Three-phase threshold capillary pressures in noncircular capillary tubes with different wettabilities including contact angle hysteresis.", *Physical Review E*, **70**(6 Pt 1), 061603 (2004).

[11] M. Piri and M.J. Blunt, "Three-dimensional mixed-wet random pore-scale network modeling of two- and three-phase flow in porous media. I. Model description", *Physical Review E*, **71** (2005).

[12] P. H. Valvatne and M. J. Blunt, "Predictive pore-scale modeling of two-phase flow in mixed wet media", *Water Resources Research*, **40**(7), (2004).

[13] P.E. Oren, S. Bakke and O.J. Arntzen, "Extending predictive capabilities to network models", *SPE J*, **3**(4), 324-336 (1998).

[14] T. W. Patzek, "Verification a complete pore network simulator of drainage and imbibition", *SPE Journal*, **6**(2), 144-156 (2001).

[15] S. Bakke and P.E. Øren, "3-D pore-scale modeling of sandstone and flow simulations in pore networks", *SPE J*, **2**(2), 136-149 (1997).

[16] Z. Jiang, K. Wu, G. Couples, M. I. J. Van Dijke, K. S. Sorbie and J. Ma, "Efficient extraction of networks from three-dimensional porous media", *Water Resources Research*, **43**(12), (2007).

[17] R. Lenormand, C. Zarcone and A. Sarr, "Mechanisms of the displacement of one fluid by another in a network of capillary ducts", *Journal of Fluid Mechanics*, **135**(OCT), 337-353 (1983).

[18] M. J. Blunt, "Physically-based network modeling of multiphase flow in intermediate-wet porous media", *Journal of Petroleum Science and Engineering*, **20**(3-4), 117-125 (1998).

[19] M. J. Oak, "Three-phase relative permeability of water-wet Berea", (*Soc of Petroleum Engineers of AIME, Richardson, TX, USA*), 109-120 (1990).